Formal Hydrogenation of a Permetalated Ethene, $(\mu_4\text{-C}{=}\text{C})Fe_2Ru_2(\eta^5\text{-}C_5Me_5)_2(CO)_8(dppm)$, via Successive Protonation−Hydride Reduction Leading to C_2H_n Cluster Compounds

Masako Terada and Munetaka Akita*

Chemical Resources Laboratory, Tokyo Institute of Technology, 4259 Nagatsuta, Midori-ku, Yokohama 226-8503, Japan

Received September 3, 2002

Formal hydrogenation of the C═C moiety in permetalated ethenes, $(\mu_4\text{-C}{=}\text{C})Fe_2Ru_2Cp^*_2(CO)_8L_2$ (Cp^*= η^5-C_5Me_5; L_2= $(CO)_2$ (**2**), dppm (**4**)), via successive addition of proton and hydride was examined. Treatment of **2** with a carboxylic acid, α-chloropropionic acid, did not result in protonation at the expected C═C moiety but addition to the Ru−Ru bond to give the μ-hydrido μ-carboxylato derivative $(\mu_4\text{-C}{=}\text{C})(\mu\text{-H})(\mu\text{-}\kappa^1{:}\kappa^1\text{-}CH_3CHClCOO)Fe_2Ru_2Cp^*_2(CO)_8$ (**3**). Irradiation of **2** in the presence of diphosphines, $Ph_2P(CH_2)_nPPh_2$ (n = 1, 2), afforded the substituted products $(\mu_4\text{-C}{=}\text{C})Fe_2Ru_2Cp^*_2(CO)_8[\mu\text{-}Ph_2P(CH_2)_nPPh_2]$ (n = 1 (**4**), 2 (**5**)), and reaction of the dppm derivative **4** with $HBF_4{\cdot}OEt_2$ resulted in protonation at the C═C moiety to give the cationic μ_4-C_2H complex $[(\mu_4\text{-C}{=}\text{CH})Fe_2Ru_2Cp^*_2(CO)_7(dppm)]BF_4$ (**6**). Further reduction of **6** with NEt_4BH_4 caused elimination of one of the iron fragments to afford the trinuclear acetylide cluster compound $(\mu_3\text{-C}{\equiv}\text{CH})FeRu_2Cp^*(CO)_5(dppm)$ (**8**), whereas treatment of **6** with H_2SiPh_2 led to H addition to provide the trinuclear μ_3-HC═CH complex $(\mu_3\text{-HC}{=}\text{CH})(\mu\text{-H})FeRu_2Cp^*(CO)_5(dppm)$ (**9**). Thus, the μ_3-HC═CH ligand in **9** arises from formal hydrogenation of the μ_4-C═C ligand in **4** (**2**) and the ligand transformations described in this paper are realized by the flexible coordination capability of the C_2 ligand. Cluster expansion by reaction of **4** with $Co_2(CO)_8$ gave the trinuclear acetylide cluster $(\mu_3\text{-C}{\equiv}\text{CFp}^*)FeRu_2CoCp^*(CO)_7(dppm)$ (**10**). Complexes **3**, **4**, **6**, and **8**−**10** have been fully characterized by means of spectroscopic and crystallographic methods.

Introduction

The organometallic chemistry of carbon allotropes ranging from one carbon atom to fullerene and carbon nanotubes has attracted increasing attention from various viewpoints, including catalytic science and material science.[1] From the former viewpoint,[2] cluster compounds containing carbon atoms have been regarded as models for surface-bound carbide species, which are key intermediates in catalytic conversions of carbon monoxide and hydrocarbons, and a number of interaction modes of carbon species with metal frameworks have been revealed so far. In contrast to the variety of coordination modes of CH_n species,[3] however, the structures and chemical properties of C_2H_n species[4,5] have remained to be studied, mainly due to the lack of appropriate synthetic precursors. The chemistry of polynuclear C_2H_n complexes (n = 0, 1) derived from the ethynyl (MC≡CH) and ethynediyl complexes (MC≡CM) bearing $Fe(\eta^5\text{-}C_5R_5)(CO)_2$ fragments has been one of our recent research activities.[4,6] In previous papers we reported the synthesis and characterization of a series of polynuclear permetalated-ethyne (**1**), -ethene (**2**), and

(1) (a) Stephens, A. H. H.; Green, M. L. H. *Adv. Inorg. Chem.* **1997**, *44*, 1. (b) Balch, A. L.; Olmstead, M. M. *Chem. Rev.* **1998**, *98*, 2123. (c) *Fullerenes: Chemistry, Physics, and Technology*, Kadish, K. M., Ruoff, R. S., Eds.; Wiley-Interscience: New York, 2000. (d) Sloan, J.; Kirkland, A. I.; Hutchinson, J. L.; Green, M. L. H. *Chem. Commun.* **2002**, 1319. (e) Paul, F.; Lapinte, C. *Coord. Chem. Rev.* **1998**, *178*−*180*, 431. (f) Low, P. J.; Bruce, M. I. *Adv. Organomet. Chem.* **2001**, *48*, 71. (g) Bartik, T.; Weng, W.; Ramsden, J. A.; Szafert, S.; Falloon, S. B.; Arif, A. M.; Gladysz, J. A. *J. Am. Chem. Soc.* **1998**, *120*, 1107. (h) Dembinski, R.; Bartik, T.; Bartik, B.; Jaeger, M.; Gladysz, J. A. *J. Am. Chem. Soc.* **2000**, *122*, 810. (i) Mohr, M.; Stahl, J.; Hampel, F.; Gladysz, J. A. *Inorg. Chem.* **2001**, *40*, 3263. (j) Stahl, J.; Bohling, J. C.; Bauer, E. B.; Peters, T. B.; Mohr, W.; Martín-Alvarez, J. M.; Hampel, F.; Gladysz, J. A. *Angew. Chem., Int. Ed.* **2002**, *41*, 1872.

(2) (a) Somorjai, G. A. *Introduction to Surface Science Chemistry and Catalysis*; Wiley-Interscience: New York, 1994. (b) Ertl, G.; Knözinger, H.; Weitkamp, J. *Handbook of Heterogeneous Catalysis*; VCH: Weinheim, Germany, 1997.

(3) (a) Tachikawa, M.; Muetterties, E. L. *Prog. Inorg. Chem.* **1981**, *28*, 203. (b) Bradley, J. S. *Adv. Organomet. Chem.* **1983**, *22*, 1. (c) Shriver, D. F.; Sailor, M. J. *Acc. Chem. Res.* **1988**, *21*, 374.

(4) (a) Akita, M.; Moro-oka, Y. *Bull. Chem. Soc. Jpn.* **1995**, *68*, 420. (b) Akita, M.; Terada, M.; Oyama, S.; Moro-oka, Y. *Organometallics* **1990**, *9*, 816. (c) Akita, M.; Terada, M.; Tanaka, M.; Moro-oka, Y. *Organometallics* **1992**, *11*, 3468. (d) Akita, M.; Hirakawa, H.; Moro-oka, Y. *Organometallics* **1995**, *14*, 2775. (e) Akita, M.; Chung, M.-C.; Sakurai, A.; Terada, M.; Miyauti, M.; Tanaka, M.; Moro-oka, Y. *J. Organomet. Chem.* **1998**, *565*, 49. (f) Akita, M.; Sugimoto, S.; Hirakawa, H.; Kato, S.; Terada, M.; Tanaka, M.; Moro-oka. M. *Organometallics* **2001**, *20*, 1555. (g) Akita, M.; Kakuta, S.; Sugimoto, S.; Terada, M.; Tanaka, M.; Moro-oka, Y. *Organometallics* **2001**, *20*, 2736.

(5) (a) Bruce, M. I. *Coord. Chem. Rev.* **1997**, *166*, 91. (b) Bruce, M. I. *J. Cluster Sci.* **1997**, *8*, 293. (c) Adams, C. J.; Bruce, M. I.; Halet, J.-F.; Kahlal, S.; Skelton, B. W.; White, A. H. *J. Chem. Soc., Dalton Trans.* **2001**, 414 and references therein. (d) Byrne, L. T.; Griffith, C. S.; Hos, J. P.; Koutsantonis, G. A.; Skelton, B. W.; White, A. H. *J. Organomet. Chem.* **1998**, *565*, 259. (e) Byrne, L. T.; Hos, J. P.; Koutsantonis, G. A.; Skelton, B. W.; White, A. H. *J. Organomet. Chem.* **1999**, *592*, 95. (f) Byrne, L. T.; Hos, J. P.; Koutsantonis, G. A.; Skelton, B. W.; White, A. H. *J. Organomet. Chem.* **2000**, *598*, 28. (g) Byrne, L. T.; Hos, J. P.; Koutsantonis, G. A.; Sanford, V.; Skelton, B. W.; White, A. H. *Organometallics* **2002**, *21*, 3147.

10.1021/om020722u CCC: $25.00
Publication on Web 12/17/2002

Scheme 1

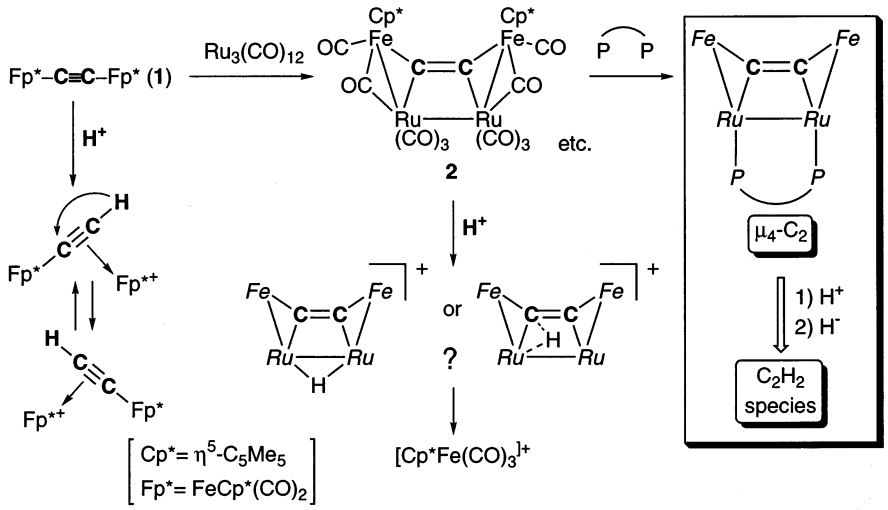

-ethane complexes,[4f] and protonation of the reactive carbon−carbon unsaturated bonds in **1** and **2** was also examined to mimic the hydrogenation process of surface-bound carbon species (Scheme 1; Cp*= η^5-C_5Me_5, Fp* = $FeCp^*(CO)_2$). Although protonation of **1** led to the formation of the cationic μ-ethynyl complex, $[Fp^*_2(\mu\text{-}C{\equiv}CH)]^+$, which showed dynamic behavior via H migration between the C_2 carbon atoms,[4b] protonation of **2** finally afforded $[Cp^*Fe(CO)_3]^+$ as the only characterizable product via fragmentation of the unstable intermediate, tentatively assigned as the protonated species, which could not be fully characterized.[4f] Herein we will describe the results of H-addition reactions to the C_2 ligand in a permetalated ethene supported by a diphosphine ligand, which is introduced to prevent fragmentation of the cluster framework. A formal hydrogenation process is mimicked by successive addition of proton and hydride,[7] and the μ_4-C_2 ligand (permetalated ethene) is successfully converted to a C_2H_2 ligand.

Results and Discussion

Protonation of Permetalated Ethene 2 Leading to Bridging Hydride Species 3. Permetalated ethene **2** was found to be basic enough to be protonated by acids such as CF_3SO_3H, HBF_4, and CF_3COOH, as we reported previously,[4f] but the product could not be fully characterized, due to the decomposition process leading to the mononuclear species $[Cp^*Fe(CO)_3]^+$ as mentioned above. We further examined protonation with weaker acids, i.e., carboxylic acids, which was monitored by ^{1}H NMR experiments in CD_2Cl_2. Upon addition of carboxylic acids characteristic ^{1}H NMR peaks around δ_H −4 were observed for all carboxylic acids examined (RCOOH; $\delta_H(\mu\text{-H})$ (R) −4.14 (CF_3), −4.10 ($CHCl_2$), −4.06 (CH_2Cl), −4.10, −4.04 ($CHClCH_3$, **3**), −3.85 (C_6H_5), −3.99 (CH_3)). This observation indicated that essentially the same reactions occurred irrespective of the carboxylic acid used, and the adduct of α-chloropropionic acid (**3**) was fully characterized (eq 1).

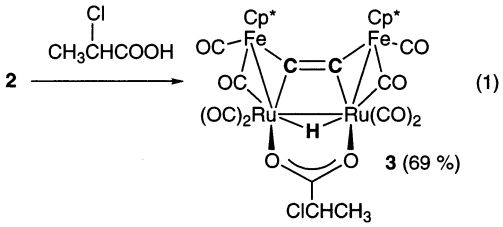

X-ray crystallography of **3** (Figure 1 and Table 1) reveals the structure arising from addition of the carboxylic acid across the Ru−Ru bond. The μ-κ^1:κ^1-carboxylato ligand is arranged perpendicular to the $(\mu_4\text{-}C_2)Fe_2Ru_2$ plane occupying the equatorial positions. (Equatorial and axial ligands refer to those arranged virtually perpendicular and coplanar, respectively, with respect to the $(\mu_4\text{-}C{=}C)Fe_2Ru_2$ plane.) The added hydrogen atom bridging the two ruthenium centers is located in the space between the axial carbonyl ligands (CO(11) and CO(15)). In accord with the location of the hydrido ligand, the Ru−Ru−CO(axial) angles for **3** (Ru2−Ru1−C3 = 113.8(2)°, Ru1−Ru2−C15 = 114.1(2)°) are considerably larger than the corresponding angle of **2** (98.7(3)°),[4f] due to steric repulsion between the hydride and axial CO ligands. Details of structural features of the core part of **3** will be discussed later, together with the diphosphine-substituted derivative.

NMR spectra of **3** (Table 2) contain two sets of signals, suggesting the formation of two isomers, which should be a pair of diastereomers arising from different combinations of the chiral carboxylato ligand (the $CHClCH_3$ part) and the apparently C_2-chiral $(\mu_4\text{-}C_2)Fe_2Cp^*_2Ru_2$ core, because the achiral carboxylic acids afforded single isomers, as indicated by the single hydride resonances. The quaternary μ_4-C_2 signals (δ_C 178.3, 178.5) are comparable to that of **2** (δ_C 177.2), and incorporation of the carboxylato ligand is verified by the corresponding NMR signals.

(6) For C_n complexes ($n = 1, \geq 3$): (a) Takahashi, Y.; Akita, M.; Moro-oka, Y. *Chem. Commun.* **1997**, 1557. (b) Akita, M.; Kato, S.; Terada, M.; Masaki, Y.; Tanaka, M.; Moro-oka, Y. *Organometallics* **1997**, *16*, 2392. (c) Akita, M.; Chung, M.-C.; Sakurai, A.; Sugimoto, S.; Terada, M.; Tanaka, M.; Moro-oka, Y. *Organometallics* **1997**, *16*, 4882. (d) Akita, M.; Sakurai, A.; Moro-oka, Y. *J. Chem. Soc., Chem. Commun.* **1999**, 101. (e) Sakurai, A.; Akita, M.; Moro-oka, Y. *Organometallics* **1999**, *18*, 3241. (f) Chung, M.-C.; Sakurai, A.; Akita, M.; Moro-oka, Y. *Organometallics* **1999**, *18*, 4684. (g) Akita, M.; Chung, M.-C.; Sakurai, A.; Sakurai, A.; Moro-oka, Y. *J. Chem. Soc., Chem. Commun.* **2000**, 1285.

(7) See for example: Cutler, A. R.; Hanna, P. K.; Vites, J. L. *Chem. Rev.* **1988**, *88*, 1363.

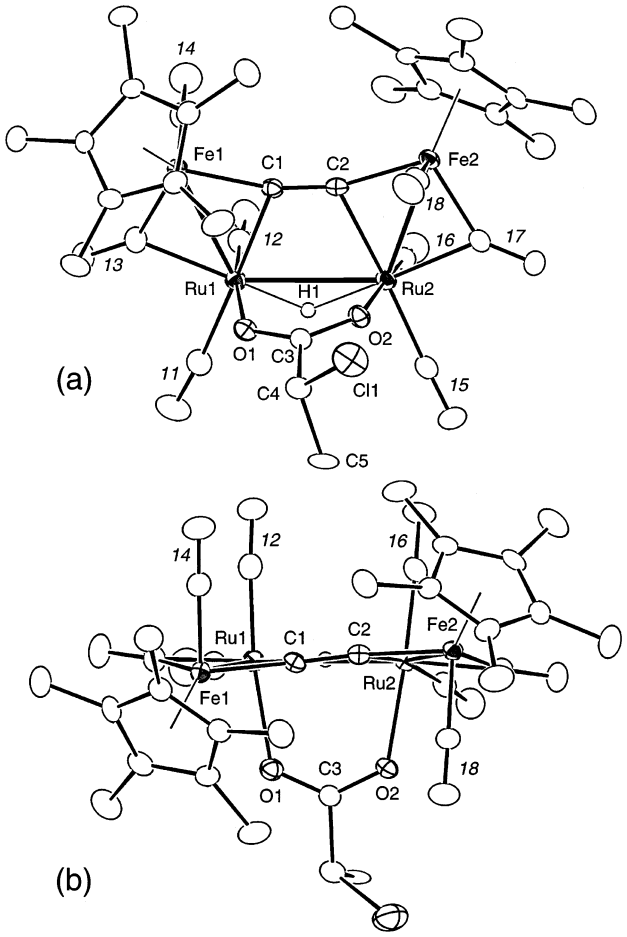

Figure 1. Molecular structure of **3**: (a) overview; (b) top view. Thermal ellipsoids are drawn at the 30% probability level. Italicized numbers are for CO ligands.

Thus, protonation of **2** with carboxylic acid results not only in protonation across the Ru−Ru bond but also in CO substitution by the nucleophilic carboxylato residue.

Synthesis of Diphosphine-Substituted Permetalated Ethenes 4 and 5. The result of the protonation experiment discussed above reveals that the μ_4-C_2 moiety in **2** is less basic than the Ru−Ru bond and the hydride species **3** results from interaction at the latter site. To increase the basicity of the C_2 moiety and reinforce the acyclic metal framework, we have examined the introduction of diphosphine ligands. In addition, if the diphosphine ligand occupies the axial coordination sites, protonation from the axial side as observed for **3** might be prevented.

Irradiation of a THF solution of a mixture of **2** and diphosphine gave the substituted products **4** and **5** (eq 2). Thermal reactions gave mixtures of products containing **4**, **5**, and the byproducts. Because the dppm complex **4** was obtained in a better yield, it was used in later studies.

Coordination of both of the phosphorus atoms in the diphosphine ligand is confirmed by the single ^{31}P NMR resonance (Table 2), which also suggests formation of a symmetrical structure: i.e., the diphosphine ligand should be coordinated to the two ruthenium atoms from the axial side in contrast to the equatorial coordination of the carboxylato ligand in **3**. Because the NMR

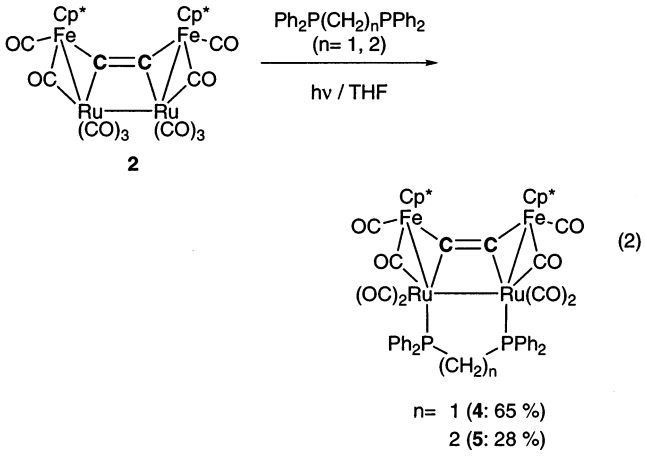

features of **4** and **5** are essentially the same as those of the starting compound **2** except for the features due to the diphosphine ligands, the symmetrical (μ_4-C_2)Fe_2Ru_2 core structure should be retained in **4** and **5**. For example, the μ_4-C_2 carbon signals (δ_C 180.9 (**4**), 182.7 (**5**); cf. **2**, δ_C 177.2) appear in the same region as triplets due to virtual coupling with the two phosphorus nuclei.

The molecular structure of the dppm complex **4** was determined by X-ray crystallography. An ORTEP drawing is shown in Figure 2, and selected structural parameters are compared with those of **2** and **3** (Table 1). The (μ_4-C_2)Fe_2Ru_2 core structures of **2**−**4** are found to be essentially the same, in accord with the results of the spectroscopic characterization. The C═C distances (1.264(7) Å (**4**), 1.270(5) Å (**3**), 1.24(1) Å (**2**)), which are close to the shorter end of C═C lengths, may suggest the contribution of triple-bond character, but the Ru−C distances of ca. 2.2 Å clearly indicate the σ-bonding interaction leading to the characterization of **2**−**4** as permetalated ethenes, although the Ru−C bonds are considerably longer. Such characterization has been also supported by MO calculations by Halet et al., as already discussed for **2**.[8] The sum of the bond angles around the μ_4-C_2 carbon atoms (359.1−359.9°) reveals the sp^2 hybridization of the μ_4-C_2 carbon atoms, and the (μ_4-C_2)-Fe_2Ru_2 moieties are planar, as can be seen from the top views (Figures 1b and 2b). The (μ_4-C_2)Fe_2Ru_2 planes in **3** and **4** are flatter than that in **2**, as judged by the Fe−Ru−Ru−Fe dihedral angles (Table 1), due to the steric constraint brought about by the μ-carboxylato and μ-dppm chelates. The two Cp* rings are projected to the opposite directions (trans) with respect to the (μ_4-C_2)-Fe_2Ru_2 plane to reduce steric repulsion between them, and the dppm ligand is arranged trans to the Fe atoms, leading to an apparent C_2-symmetrical structure consistent with the spectroscopic features.[9]

Protonation of Phosphine-Substituted Permetalated Ethene 4 To Give the μ_4-C_2H Complex 6. The μ_4-C_2 complex **4** was subjected to protonation with HBF_4·OEt_2 and, as a result, the dark brown product **6** was isolated in 64% yield (Scheme 2). Appearance of the

(8) (a) Frapper, G.; Halet, J.-F. Bruce, M. I. *Organometallics* **1995**, *14*, 5044. (b) Frapper, G.; Halet, J.-F. Bruce, M. I. *Organometallics* **1997**, *16*, 2590.

(9) Similar structural characteristics of the permetalated ethenes were noted for the tetraruthenium derivatives (μ_4-C═C)Ru_4(η^5-C_5H_4R)$_2$-$(CO)_{10}$, recently reported by Kousantonis, although the cis isomer was also formed in the case of the sterically less congested η^5-C_5H_5 derivative.[5f]

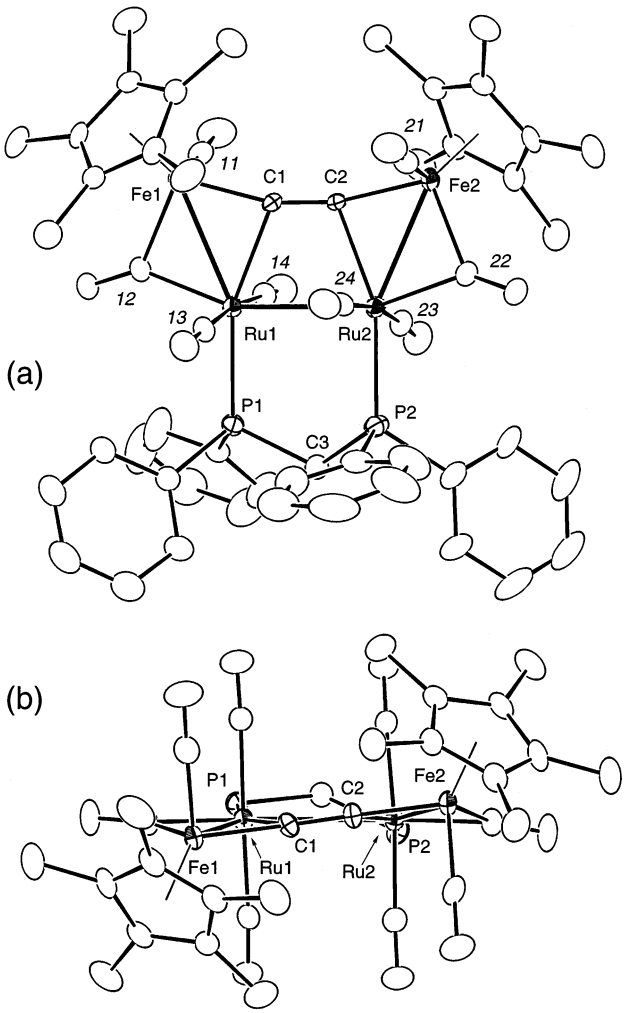

Figure 2. Molecular structure of **4**: (a) overview; (b) top view. Thermal ellipsoids are drawn at the 30% probability level. Italicized numbers are for CO ligands.

singlet ^{1}H NMR signal at δ_H 10.71 and the ν_{BF} vibration suggested the occurrence of protonation (Table 2). The ^{13}C NMR signals for the C_2H moiety were located at δ_C 153.7 (dd, J_{PC} = 36.1 Hz, $^1J_{CH}$ = 178.2 Hz) and 301.7 (dd, J_{PC} = 22.0 Hz, $^2J_{CH}$ = 7.0 Hz), which were assigned on the basis of the magnitude of the C−H coupling constants, and the assignments were definitely confirmed by HMQC and HMBC 2D(C−H) NMR techniques. These spectroscopic data verified the formation of a C_2H functional group via protonation at the μ_4-C_2 ligand in **4** but did not provide any information concerning the metal framework, which was characterized by X-ray crystallography.

The molecular structure of **6** is shown in Figure 3, and selected structural parameters are listed in Table 3. First of all, the formation of a μ_4-C_2H ligand is evident. As for the arrangement of the metal atoms, the acyclic Fe_2Ru_2 linkage in **4** is converted to the out-of-plane spiked triangular metal array, with which the C_2H ligand is bonded through three σ bonds (Fe1, Ru1, Ru2) and one π bond (Fe2). Previous studies revealed two types of coordination modes of an acetylide ligand to a spiked triangular metal array, i.e., ∥ and ⊥ modes (Chart 1), which are characterized by the orientation of the acetylide ligand with respect to the basal metal triangle and the extent of the bonding interaction

Table 1. Comparison of Structural Parameters for Permetalated Ethenes 2−4

	3[a]	**4**	**2**[b]
	Bond Lengths (Å)		
C1 −C2	1.263(7)	1.270(5)	1.24(1)
Fe1−C1	1.923(4)	1.925(4)	1.946(7)
Fe2−C2	1.923(5)	1.921(4)	1.946(7)
Ru1−C1	2.173(5)	2.202(4)	2.204(7)
Ru2−C2	2.180(4)	2.183(4)	2.204(7)
Ru1−Ru2	2.9624(5)	2.9511(5)	2.963(2)
Ru1−Fe1	2.741(1)	2.7012(6)	2.733(2)
Ru2−Fe2	2.708(1)	2.6797(7)	2.733(2)
Ru1−X (X)	2.160(4) (O1)	2.319(1) (P1)	
	2.142(3) (O2)	2.306(1) (P2)	
	Bond Angles (deg)		
Ru1−C1−C2	109.8(3)	113.3(3)	112.0(2)
Ru2−C2−C1	115.6(4)	110.8(3)	112.0(2)
Fe1−C1−C2	166.3(4)	165.0(3)	165.5(2)
Fe2−C2−C1	161.1(4)	167.7(3)	165.5(2)
Ru1−C1−Fe1	83.8(2)	81.5(2)	82.1(2)
Ru2−C2−Fe2	82.4(2)	81.2(1)	82.1(2)
Fe1−Ru1−C1	44.2(1)	44.8(1)	44.9(2)
Fe2−Ru2−C2	44.7(1)	45.1(1)	44.9(2)
Ru2−Ru1−C1	68.2(1)	66.4(1)	66.5(2)
Ru1−Ru2−C2	65.5(1)	68.1(1)	66.5(2)
Ru1−Fe1−C1	52.0(1)	53.7(1)	53.0(2)
Ru2−Fe2−C2	52.9(1)	53.6(1)	53.0(2)
Ru2−Ru1−Fe1	112.26(2)	110.92(2)	110.61(4)
Ru1−Ru2−Fe2	110.26(2)	112.98(2)	110.61(4)
	Dihedral Angle (deg)		
Fe1−Ru1−Ru2−Fe2	9.56(3)	15.40(2)	24

[a] Ru1−H1 = 1.56(7) Å, Ru2−H1 = 1.70(6) Å. [b] A C_2-symmetrical molecule. The corresponding values are listed.[4f]

Chart 1

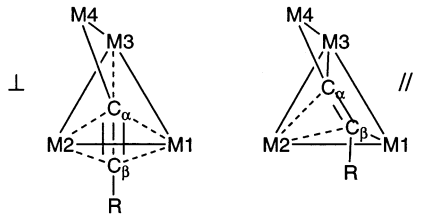

Scheme 2

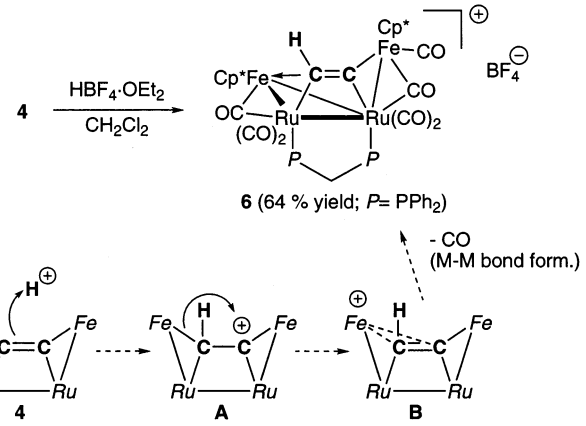

between C_α and M1.[4,10] The μ_4-C_2H complex **6** belongs to the latter category, as judged by the C1···Ru2 separation (2.79(1) Å) exceeding the range of a bonding interaction. The related μ_4-∥-C_2H and μ_4-⊥-C_2H tetranuclear cluster compounds (μ_4-∥-C_2H)$FeCo_2Ru(\eta^5$-$C_5R_5)$-$(CO)_{10}$ (**7**; δ_C(CH) 160.7 (J_{CH} = 193 Hz), δ_C(C) 198.9),[4d] (μ_4-⊥-C_2H)$FeNi_3(\eta^5$-$C_5R_5)Cp_2(CO)_3$,[4c] and (μ_4-⊥-C_2H)-$Fe_2Co_2(\eta^5$-$C_5R_5)(CO)_9$[4e] were obtained from the ethynyl complexes (η^5-C_5R_5)$(CO)_2FeC{\equiv}CH$ (R= H, Me) and

Table 2. Selected Spectroscopic Data for C_2H_n Cluster Compounds

complex[a]	^{1}H NMR (δ_H)[b] CH	^{1}H NMR (δ_H)[b] Cp*	^{31}P NMR (δ_P)[b]	^{13}C NMR (δ_C)[b] C_2H_n	^{13}C NMR (δ_C)[b] C_5Me_5	^{13}C NMR (δ_C)[b] CO	IR (KBr, ν_{CO}/cm^{-1})
2[c,d] (C_6D_6)		1.55		177.2	98.0, 9.5	191.1, 196.4, 205.6, 217.8, 262.5	2082, 2048, 1997, 1981, 1963, 1953, 1775
3[d] (CD_2Cl_2)	−4.04,[e] −4.10[e]	1.82, 1.83, 1.94		178.3, 178.5	98.7, 99,4, 99.3, 9.2, 9.3, 9.5	*d*	2041, 2026, 1980, 1953, 1792, 1653, 1570
4 (CD_2Cl_2)		1.90	48.9	180.9 (t, 12.2)[f]	96.8, 9.6	197.0 (t, 7.3), 205 (t, 7.3), 215.1, 272.2	2010, 1948, 1931, 1774, 1757
5 (CD_2Cl_2)		1.89	43.3	182.7 (d, 22.0)	97.3, 9.8	195.8 (d, 17.1), 206.2 (d, 17.1), 215.4, 273.9	2003, 1936, 1754
6 ($CDCl_3$)	10.71	1.91, 1.64	46.3 (d, 7.6),[g] 33.2 (d, 7.6)[g]	153.7 (dd, 178.2, 36.1[f]), 301.7 (dd, 7.0, 22.0[f])	100.7, 96.7, 9.2, 9.1	194.2, 197.5, 204.8, 208.5, 211.5, 212.2, 256.3, 262.8	2049, 1980, 1958, 1908, 1783, 1752, 1640
8 (C_6D_6)	8.68	1.75	44.3 (d, 70),[g] 40.8 (d, 70)[g]	112.2 (d, 214.9), 300.0 (d, 4.8)		199.7, (d, 7.3), 200.5, 206.1, 206.6, 243.9	1993, 1964, 1939, 1917, 1805
9[h] (C_6D_6)	9.20 (2H, t, 4.7)[i]	1.74	42.1	155.1 (d, 153.8)	92.5, 9.4	271.0, 202.4, 201.1	2006, 1997, 1957, 1942, 1677
10 (CD_2Cl_2)		1.83	24.4	*j*	97.8, 10.1	214.2[j]	2028, 2006, 1974, 1943, 1917, 1872, 1848

[a] Solvents for NMR measurements are shown in parentheses. [b] ^{1}H (400 MHz), ^{13}C (100 MHz), and ^{31}P NMR spectra (81 MHz) were recorded at ambient temperature. Signals are singlets unless otherwise stated, and coupling constants (J_{CH} unless otherwise stated) are shown in parentheses. The $\delta_C(C_5Me_5)$ signals around 10 ppm are quartets with J_{CH} = 127−129 Hz. [c] Reference 4f. [d] **3**: a mixture of two diastereomers, δ^C(CO) 200.6, 200.8, 201.8, 201.9, 202.4 (d, 6.5), 202.5 (d, 6.5), 202.8 (d, 6.5), 202.9 (d, 6.5), 209.6, 210.9, 259.9 (d, 8.6), 260.0 (d, 8.6), 266.2 (d, 6.4), 266.3 (d, 6.4). [e] μ-H signals. [f] J_{PC}. [g] J_{PP}. [h] $\delta_H(\mu$-H) −16.85 (1H, t, J_{PH} = 15.7 Hz). [i] J_{PH}. [j] A satisfactory data set could not be obtained, due to low solubility in organic solvents.

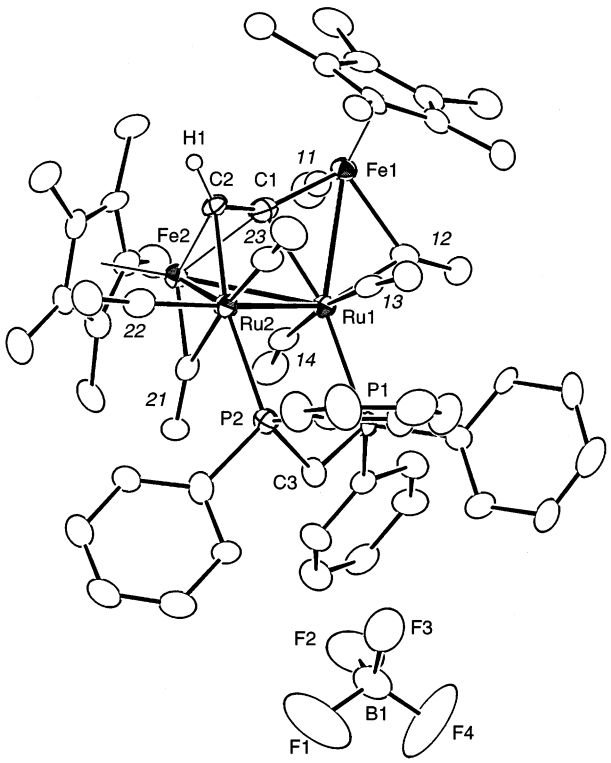

Figure 3. Molecular structure of **6**. Thermal ellipsoids are drawn at the 30% probability level. Italicized numbers are for CO ligands.

trinuclear metal carbonyl species, as we reported previously. When the ^{13}C NMR data for the C_2H parts of the ||-type complexes **6** and **7** are compared, the smaller $^1J_{CH}$ value for **6** indicates an increased contribution of the || form containing the sp^2-hybridized CH moiety. In accord with this consideration the α-carbon signal of **6** (δ_C 301.7) appears in the highly deshielded region typical for α-carbon signals of polynuclear μ-vinylidene complexes,[11] and such an olefinic structure should result from effective back-donation from the electron-donating Ru−P fragments to the π* orbital of the C≡CH part.

A plausible formation mechanism for **6** is delineated in Scheme 2. Judging from the structure of **6**, the initial protonation should occur at the μ_4-C_2 moiety in **4** to give the carbocationic C_2H intermediate **A**. Subsequent interaction of the carbocationic center with the distal iron center should lead to the η^2-coordinated intermediate **B**, which is finally converted to **6** with the spiked triangular metal array via decarbonylation associated with metal−metal bond formation. The driving force for the rearrangement of the cationic species should be the difference in their relative stabilities. The carbon-centered cationic species **A** could be stabilized by back-donation from the two σ-bonded metal centers, but the final product **6**, where the cationic charge is spread widely over the tetranuclear metal array, should be more stable than **A**. Thus, the introduction of the dppm ligand has changed the protonation site and the expected C_2H species **6** has been obtained successfully.

Hydride Reduction of μ_4-C_2H Cluster Compound 6. (i) Reduction with NEt_4BH_4 To Give the Trinuclear C_2H Cluster Compound 8. The cationic C_2H cluster compound **6** was further subjected to hydride

(10) (a) Sappa, E.; Tiripicchio, A.; Braunstein, P. *Chem. Rev.* **1983**, *83*, 203. (b) Sappa, E.; Tiripicchio, A.; Carty, A. J.; Toogood, G. E. *Prog. Inorg. Chem.* **1987**, *35*, 437. (c) Raithby, P. R.; Rosales, M. J. *Adv. Inorg. Chem. Radiochem.* **1985**, *29*, 169. (d) Carty, A. J. *Pure Appl. Chem.* **1982**, *54*, 113. (e) *Comprehensive Organometallic Chemistry II*; Abel, E. W., Stone, F. G. A., Wilkinson, G., Eds.; Pergamon: Oxford, U.K., 1995; Vol. 7, Chapter 4.
(11) Bruce, M. I. *Chem. Rev.* **1998**, *98*, 2797.

Table 3. Selected Structural Parameters for C_2H_n Cluster Compounds

Bond Lengths (Å)

	6[a]	**8**[b]	**9**[c]	**10**
C1−Fe1	1.93(1)	2.036(6)	2.009(6)	1.958(4)
C1−M (M)	2.07(1) (Fe2)			2.318(4) (Co1)
C1−Ru1	2.12(1)	2.179(5)	2.091(6)	2.431(4)
C1−Ru2				
C2−Fe1	2.07(1)	2.063(4)	1.999(6)	
C2−Fe2	2.02(1)			
C2−Ru1			2.217(4)	2.245(3)
C2−Ru2	2.141(9)	1.957(5)	2.100(5)	2.043(3)
C2−M (M)			2.100(5)	2.098(3) (Co1)
M−M	2.838(1) (Ru1−Ru2)	2.8053(5) (Ru1−Ru2)	2.8789(4) (Ru1−Ru2)	2.7972(3) (Ru1−Ru2)
	2.693(1) (Ru1−Fe1)	2.6355(6) (Ru1−Fe1)	2.7054(8) (Ru1−Fe1)	2.5994(6) (Ru1−Co1)
	2.810(2) (Ru1−Fe2)	2.7789(6) (Ru2−Fe1)	2.7034(7) (Ru2−Fe1)	2.6458(5) (Ru2−Co1)
	2.616(2) (Ru2−Fe2)			
Ru1−P1	2.374(3)	2.287(1)	2.417(2)	2.3243(9)
Ru2−P2	2.402(3)	2.307(1)	2.388(1)	2.2956(9)

Bond Angles (deg)

Compound 6							
Ru2−Ru1−Fe1	108.32(4)	Ru1−Fe2−Ru2	62.96(4)	Fe1−C1−Fe2	139.5(6)	Ru2−C2−C1	104.1(7)
Ru2−Ru1−Fe2	55.18(4)	Ru1−C1−Fe1	83.2(5)	Fe1−C1−C2	149.6(9)	Fe2−C2−C1	72.8(7)
Fe1−Ru1−Fe2	85.90(5)	Ru1−C1−Fe2	84.1(4)	Fe2−C1−C2	68.8(6)	C1−Fe2−C2	38.4(4)
Ru1−Ru2−Fe2	61.86(4)	Ru1−C1−C2	117.0(7)	Ru2−C2−Fe2	77.8(3)		
Compound 8							
Ru2−Ru1−Fe1	61.33(1)	Ru1−C1−C2	74.1(3)	Ru1−C2−C1	71.0(3)	Fe1−C2−C1	70.1(3)
Ru1−Ru2−Fe1	56.32(1)	Fe1−C1−C2	72.4(3)	Ru2−C2−Fe1	87.4(2)	C1−Ru1−C2	34.9(2)
Ru1−Fe1−Ru2	62.35(2)	Ru1−C2−Ru2	84.2(2)	Ru2−C2−C1	149.7(4)	C1−Fe1−C2	37.5(2)
Ru1−C1−Fe1	77.3(2)	Ru1−C2−Fe1	75.9(1)				
Compound 9							
Ru2−Ru1−Fe1	57.81(2)	Ru1−C1−Fe1	82.6(2)	Ru2−C2−Fe1	82.5(2)	Fe1−C2−C1	69.9(3)
Ru1−Ru2−Fe1	57.88(2)	Ru1−C1−C2	111.8(4)	Ru2−C2−C1	109.4(4)	C1−Fe1−C2	41.0
Ru1−Fe1−Ru2	64.32(2)	Fe1−C1−C2	69.1(3)				
Compound 10							
Ru2−Ru1−Co1	58.58(1)	Ru1−C1−C2	66.3(2)	Ru1−C2−Ru2	81.3(1)	Ru2−C2−C1	159.0(3)
Ru1−Ru2−Co1	56.97(1)	Co1−C1−Fe1	124.4(2)	Ru1−C2−Co1	73.4(1)	Co1−C2−C1	83.1(2)
Ru1−Co1−Ru2	64.45(1)	Co1−C1−C2	64.0(2)	Ru1−C2−C1	82.6(2)	C1−Ru1−C2	31.2(1)
Ru1−C1−Co1	66.3(1)	Fe1−C1−C2	161.5(3)	Ru2−C2−Co1	79.4(1)	C1−Co1−C2	32.9(1)
Ru1−C1−Fe1	131.3(2)						

[a] C2−H1 = 0.97(6) Å. [b] C1−H1 = 1.21(7) Å. [c] C1−H1 = 1.15(7) Å, C2−H2 = 1.10(7) Å, Ru1−H3 = 1.83(6) Å, Ru2−H3 = 1.95(5) Å.

Scheme 3

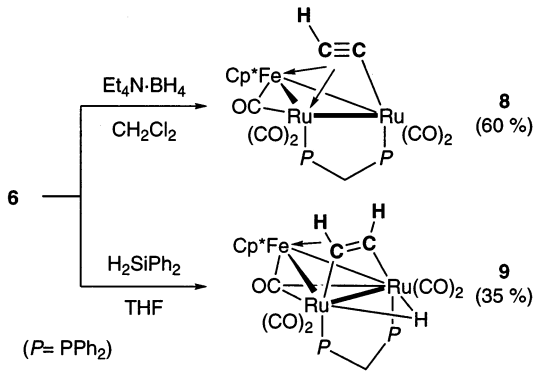

reduction to add more hydrogen atoms (Scheme 3). Treatment of **6** with Et_4NBH_4 in CH_2Cl_2 gave the red-brown product **8** after chromatographic separation. The NMR data ($\delta_H(C_2H)$ 8.68; $\delta_C(C_\alpha)$ 300.0 (d, J_{CP} = 4.8 Hz), $\delta_C(C_\beta)$ 111.2 (d, J_{CH} = 214.9 Hz)), in particular, the highly deshielded C_α signal and the large C−H coupling constant of the C_β signal, suggested formation of an ethynyl cluster compound. X-ray crystallography of **8** (Figure 4 and Table 3) revealed a typical trinuclear μ_3-η^1:η^2:η^2-ethynyl cluster-type structure,[10] which should result from removal of one of the Cp*Fe$(CO)_n$ fragments in **6**. The hydride attacked presumably at the π-bonded iron center rather than at the C_2H ligand, and actually,

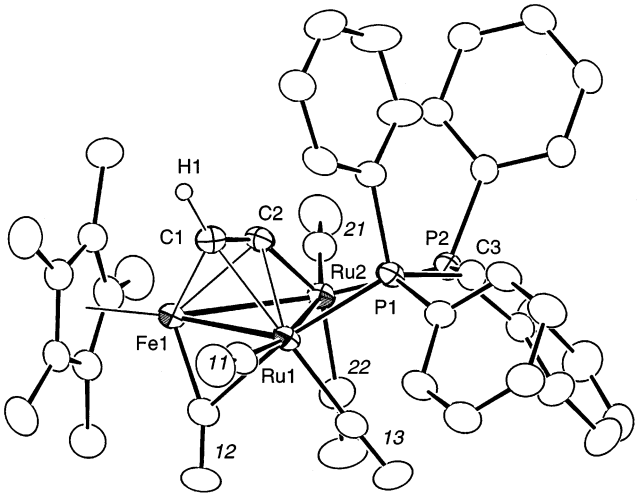

Figure 4. Molecular structure of **8**. Thermal ellipsoids are drawn at the 30% probability level. Italicized numbers are for CO ligands.

a substantial amount of Fp^*_2, which should be formed via oxidative dimerization of Fp−H, was obtained as the major byproduct.

(ii) Reduction with H_2SiPh_2. We expected that reduction of **6** with hydrosilane, a milder reducing agent, could change the reaction pathway.[12]

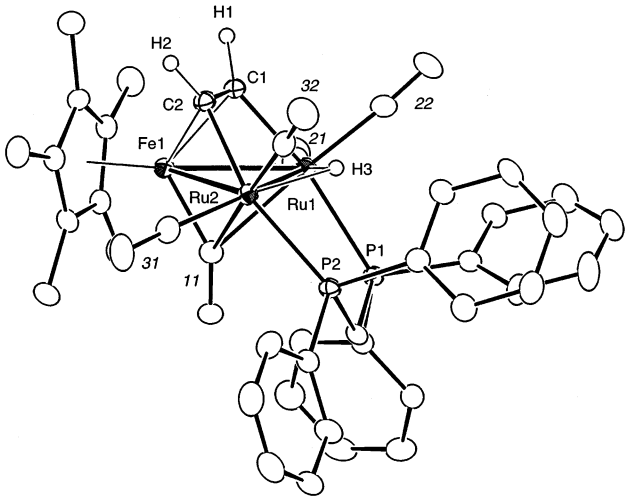

Figure 5. Molecular structure of **9**. Thermal ellipsoids are drawn at the 30% probability level. Italicized numbers are for CO ligands.

Scheme 4

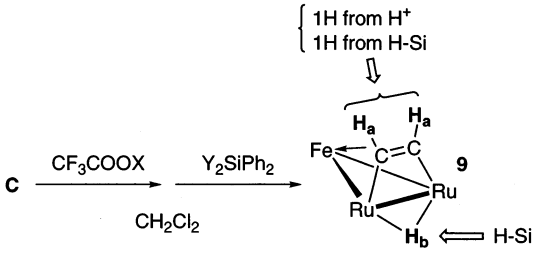

X in CF_3COOX	Y in Y_2SiPh_2	the extent of deuteration	
		H_a	H_b
H	D	0.98	0.97
D	H	1.38	0.95
D	D	1.96	0.86

Treatment of **6** with H_2SiPh_2 gave the purple product **9** in a moderate yield. Characteristic NMR features of **9** are (i) the olefinic proton signal with the intensity 2H, (ii) the hydride resonance (δ_H −16.85 (1H, t, J = 15.7 Hz)), (iii) the presence of only one Cp* ring, and (iv) the single ^{31}P resonance, suggesting formation of a mirror-symmetrical structure resulting from loss of one of the two $Cp^*Fe(CO)_n$ groups in **6**. X-ray crystallography (Figure 5 and Table 3) revealed the trinuclear μ_3-||-alkyne cluster-type structure[10] with a bridging hydride ligand, which was consistent with the NMR features. The C═C distance is the longest of the C_2H_n complexes appearing in this paper, as is consistent with the reduction of the acetylenic C≡C functional group to an olefinic C═C group. Treatment of the C_2H cluster **8** with H_2SiPh_2 did not result in conversion to **9**.

Thus, two hydrogen atoms are incorporated during reduction of **6** and the source of the hydrogen atoms in **9** was confirmed by labeling experiments (Scheme 4). The μ_4-C_2 complex **4** was treated successively with CF_3COOX and Y_2SiPh_2 (X, Y = H, D), and the resultant mixture was analyzed by ^1H NMR after removal of the volatiles under reduced pressure. Formation of the protonated intermediate [(μ_3-C═CH)$Fe_2Ru_2Cp^*(CO)_7$]-

(12) $HSnR_3$ also reacted with **6**, but no characterizable product could be obtained.

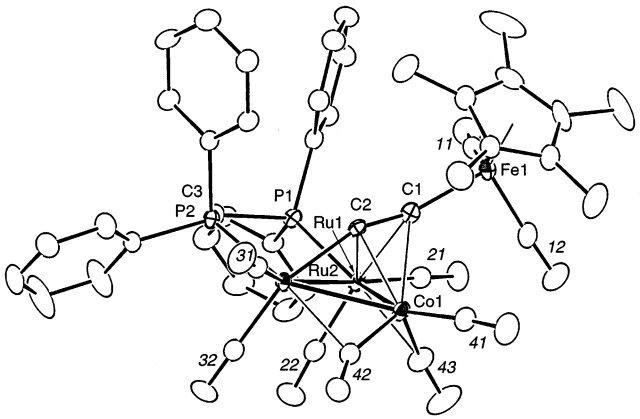

Figure 6. Molecular structure of **10**. Thermal ellipsoids are drawn at the 30% probability level. Italicized numbers are for CO ligands.

CF_3COO, analogous to **6**, was confirmed by an NMR experiment; addition of CF_3COOH to a CD_2Cl_2 solution of **4** gave ^1H and ^{31}P spectra (δ_H 10.60 (1H, s, C_2H), 1.95, 1.63 (15H × 2, s × 2, 2Cp*); δ_P 45.7, 32.8 (d × 2, J = 76 Hz)) similar to those of **6** (Table 2). The results of the deuteration experiments summarized in Scheme 4 reveal that one of the two olefinic hydrogen atoms (H_a) comes from the acid proton and the other olefinic hydrogen atom (H_a) and the hydride atom (H_b) come from diphenylsilane.

The μ_4-C_2H_2 complex **9** should be formed via a sequence involving (i) hydride transfer to the C_2H ligand in **6**, (ii) oxidative addition of the Si−H bond in diphenylsilane, and (iii) elimination of an Fe−Si fragment. Thus, formal hydrogenation of the permetalated ethene **4** (**2**) has been achieved.

Attempted Expansion of 4 by Treatment with $Co_2(CO)_8$. Cluster expansion of **4** was attempted by addition of metal carbonyl fragments.[5] Reaction of **4** with $Co_2(CO)_8$ in hot benzene gave the purple product in an almost quantitative yield after chromatographic separation (eq 3).

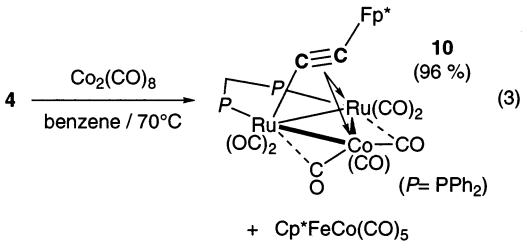

A ^1H NMR spectrum of **10** revealed the presence of both the Cp* and dppm ligands, but the low solubility of **10** in organic solvents hampered collection of a satisfactory ^{13}C NMR data set. Then **10** was subjected to X-ray crystallography. The molecular structure of **10** is shown in Figure 6, and selected structural parameters are listed in Table 3. Complex **10** is thus characterized as a trinuclear μ_3-η^1(Ru1):η^2(Ru2):η^2(Co1)-acetylide cluster compound, and the structural features of the core similar to those of **8** are normal for such a type of cluster compound.[10]

It is notable that the olefinic permetalated ethene structure (μ_4-C═C)Fe_2Ru_2 in **4** is converted to the acetylenic functional group (Fp*C≡C) in **10**. Both the

starting compound **4** and the product **10** are tetranuclear 66-CVE (cluster valence electron) species. Formal replacement of the 13e Cp*Fe fragment in **4** by the 11e Co(CO) fragment leads to **10**, and accordingly, during this process the C_2 moiety changes from a 4e donor (4σ) to a 6e donor ($2\sigma + 2\pi$). The FeC═C group in **4** is interconvertible with the FeC≡C group, and this intriguing behavior may originate from the flexibility of possible coordination modes of the C_2 ligand, as shown in Chart 2.

Chart 2

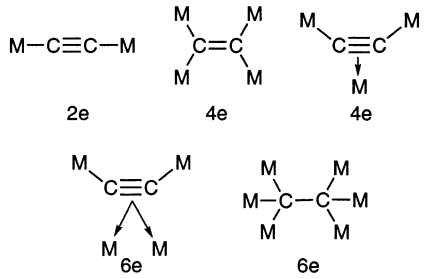

Formation of **10** can be interpreted in terms of Scheme 5. Initial isolobal replacement of the FeCp*(CO)

Scheme 5

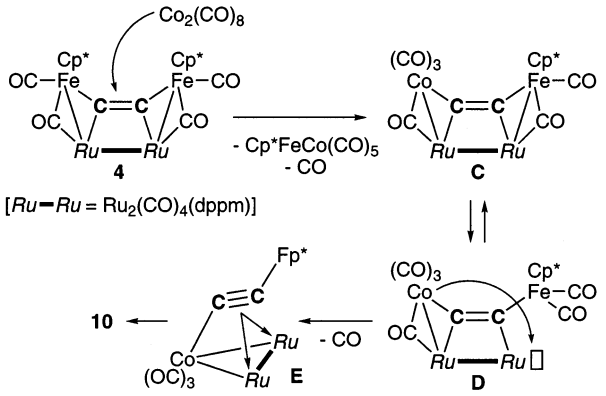

fragment by the $Co(CO)_3$ fragment through interaction between the μ_4-C═C moiety and $Co_2(CO)_8$ should give the Co-substituted permetalated ethene intermediate **C**, which should be in equilibrium with the coordinatively unsaturated species **D** via bridge-to-terminal migration of the bridging CO ligand accompanied by metal−metal bond scission. Electron donation from the Co moiety to the unsaturated Ru moiety followed by reorganization of the coordination mode of the C≡C part furnishes the acetylide cluster species **E**, which is finally converted to **10** via rotation of the C≡CFp* group over the Ru_2Co face.

Conclusion

The cluster transformations described in this paper, i.e., formal hydrogenation of a permetalated ethene **4** (**2**) via successive addition of H^+ and H^-, are summarized in Scheme 6. Treatment of the parent permetalated ethene **2** with carboxylic acids results in protonation across the Ru−Ru bond from the axial side (**3**) rather than the expected H addition to the μ_4-C_2 ligand. Photochemical substitution of **2** by diphosphines affords the chelated products **4** (dppm) and **5** (dppe) with virtual C_2 symmetry. Upon treatment with $HBF_4{\cdot}OEt_2$, the dppm-substituted derivative **4** is converted to the cationic C_2H complex (**6**) with a spiked triangular metal array via protonation and decarbonylation associated with metal−metal bond formation. Borohydride reduction of **6** causes elimination of one of the iron fragments, whereas treatment of **6** with H_2SiPh_2 affords the μ_3-HC═CH complex **9** via formal hydrogenation of the μ_4-C═C moiety in **2** (**4**). Reaction of the dppm complex **4** with $Co_2(CO)_8$ produces the trinuclear acetylide cluster **10** via conversion of the FeC═C linkage into the FeC≡C functional group.

The results suggest the occurrence of an analogous hydrogenation process of a C_2 species on a metallic surface, and the cluster transformations are realized by virtue of the flexible coordination behavior of the C_2 ligand. Reactivity of permetalated ethenes including **2** and **4** is now under further study, and results will be reported in due course.

Scheme 6

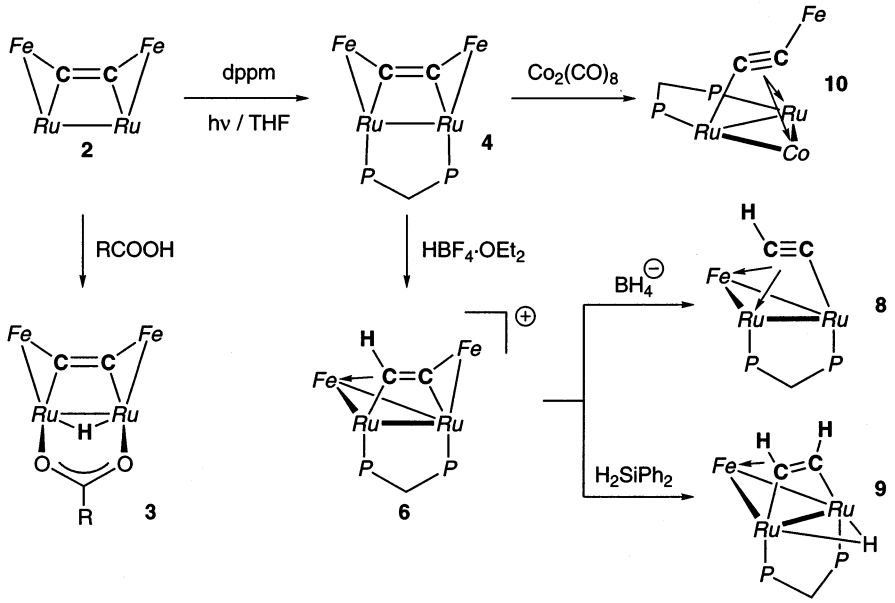

Experimental Section

General Methods. All manipulations were carried out under an inert atmosphere by using standard Schlenk tube techniques. THF, ether, hexanes, benzene, toluene (Na−K alloy), CH_2Cl_2 (P_2O_5), and EtOH ($Mg(OEt)_2$) were treated with appropriate drying agents, distilled, and stored under argon. ^1H and ^{13}C NMR spectra were recorded on Bruker AC-200 (^1H, 200 MHz; ^{31}P, 81 MHz) and JEOL EX-400 spectrometers (^{13}C, 100 MHz). Solvents for NMR measurements containing 0.5% TMS were dried over molecular sieves, degassed, distilled under reduced pressure, and stored under Ar. IR spectra (KBr pellets) and mass spectra (FD) were obtained on a JASCO FT/IR 5300 spectrometer and a Hitachi M-80 mass spectrometer, respectively. Complex **2** was prepared according to the published method.[4g] Other chemicals were purchased and used as received. Chromatography was performed on alumina unless otherwise stated.

Reaction of 2 with $CH_3CHClCOOH$ To Give 3. To a stirred CH_2Cl_2 solution (6 mL) of **2** (178 mg, 0.20 mmol) was added $CH_3CHClCOOH$ (80 μL, 0.94 mmol). After 1 h the mixture was subjected to Florisil column chromatography. The band of Fp^*_2 was eluted with 1:3 Et_2O−hexane, and a purple band eluted with Et_2O was collected. Removal of the volatiles and crystallization of the residue from CH_2Cl_2−hexane gave **3** (130 mg, 0.14 mmol, 69% yield) as dark purple crystals. **3**: ^1H NMR (CD_2Cl_2) δ_H 3.48, 3.23 (1H × 2, q × 2, J = 6.8 Hz, CHCl), 0.96, 0.86 (3H × 2, d × 2, J = 6.8 Hz, CH_3); ^{13}C NMR (CD_2Cl_2) δ_C 192.3 (d, J = 4.3 Hz, COO), 55.4, 55.0 (dq × 2, J = 152.6, 4.3 Hz, CHCl), 21.8, 21.1 (q × 2, J = 131.1 Hz, CH_3). Anal. Calcd for $C_{33}H_{35}O_{10}ClFe_2Ru_2$: C, 3.72; H, 3.72; Cl, 3.77. Found: C, 42.04; H, 3.92; Cl, 3.70.

Preparation of 4. A THF solution (500 mL) of a mixture of **2** (726 mg, 0.82 mmol) and dppm (565 mg, 1.47 mmol) cooled in an ice−water bath was irradiated by a high-pressure Hg lamp for 13 h. After removal of the volatiles the residue was subjected to alumina column chromatography. Elution with CH_2Cl_2−hexane (1:5−1:1) gave a purple band, from which **4** (686 mg, 0.56 mmol, 65% yield) was isolated after removal of the eluent and crystallization from ether−hexane. **4**: ^1H NMR ($CDCl_3$) δ_H 8.34−8.29, 7.63−7.61, 7.38, 7.10−7.07 (20H, m, Ph), 4.22 (2H, t, J = 10.4 Hz, CH_2); ^{13}C NMR (CD_2Cl_2) δ_C 140.3, 136.5, 134.1, 130.6, 130.3, 129.1, 128.8, 127.9 (Ph), 47.4 (t, J_{CP} = 32 Hz, CH_2). Anal. Calcd for $C_{61}H_{66}O_8P_2Fe_2Ru_2$ (**1**·(hexane)): C, 56.23; H, 5.11. Found: C, 55.93; H, 4.95.

Preparation of 5. The dppe complex **5** was prepared from **2** and dppe in a manner similar to the preparation of **4**. **5** (28% yield; dark purple crystals): ^1H NMR (CD_2Cl_2) δ_H 8.37−8.27, 7.63−7.52, 7.25−7.21 (20H, m, Ph), 3.67−3.53 (4H, m, $(CH_2)_2$); ^{13}C NMR (CD_2Cl_2) δ_C 141.0, 134.0, 133.6, 130.9, 129.8, 129.0, 128.4 (Ph), 25.3 (t, J_{CP} = 32 Hz, CH_2). Anal. Calcd for $C_{56}H_{54}O_8P_2Fe_2Ru_2$: C, 54.66; H, 4.39. Found: C, 54.68; H, 4.70.

Preparation of 6: Protonation of 4. To a CH_2Cl_2 solution (20 mL) of **4** (487 mg, 0.40 mmol) immersed in an ice−water bath was added HBF_4·OEt_2 (0.1 mL, 0.80 mmol), and the resultant mixture was stirred for 1 h at ambient temperature. After filtration through a Celite plug and concentration ether was added to the filtrate. Addition of ether gave a white solid contaminated with dark brown species, which was discarded. Further addition of ether gave **6** (324 mg, 0.25 mmol, 64% yield) as dark brown crystals. **6**: ^1H NMR ($CDCl_3$) δ_H 7.91−6.58 (20H, m, Ph), 3.74 (2H, br, CH_2); ^{13}C NMR ($CDCl_3$) δ_C 135.9 (m, ipso), 135.5 (m, ipso), 134.7 (dd, J_{CP} = 12.2, J_{CH} = 161.1 Hz), 133.7 (dd, J_{CP} = 12.2 Hz, J_{CH} = 161.1 Hz), 131.9 (dd, J_{CP} = 23.3 Hz, J_{CH} = 163.0 Hz), 131.1 (dd, J_{CP} = 9.8 Hz, J_{CH} = 163.6 Hz), 130.4 (dd, J_{CP} = 9.8 Hz, J_{CH} = 163.5 Hz), 129.8 (dd, J_{CP} = 9.8 Hz, J_{CH} = 166.0 Hz), 129.3 (dd, J_{CP} = 9.8 Hz, J_{CH} = 163.5 Hz), 128.8 (dd, J_{CP} = 9.8 Hz, J_{CH} = 163.5 Hz), 128.4 (dd, J_{CP} = 9.8 Hz, J_{CH} = 163.5 Hz), 30.6 (tt, J_{CP} = 24 Hz, J_{CH} = 129 Hz, CH_2). Anal. Calcd for $C_{54}H_{53}BF_4O_7P_2Fe_2Ru_2$: C, 50.81; H, 4.18. Found: C, 50.82; H, 4.26.

Preparation of 8: NEt_4BH_4 Reduction of 6. To a THF solution (12 mL) of **6** (357 mmol, 0.27 mmol) was added NEt_4BH_4 (320 mg, 1.10 mmol) in portions, and the resultant mixture was stirred for 6 h at room temperature. After removal of the volatiles under reduced pressure the residue was extracted with ether and the extract passed through an alumina plug. Separation by column chromatography (eluted with 1:1 Et_2O−hexane) gave **8** as dark red-brown crystals (212 mg, 0.17 mmol, 64% yield). **8**: ^1H NMR (C_6D_6) δ_H 7.76−6.82 (20H, m, Ph), 3.70−3.60 (2H, br, CH_2); ^{13}C NMR (C_6D_6) δ_C 129.6 (d, J_{CP} = 14.6 Hz), 129.7 (d, J_{CP} = 14.6 Hz), 131.0 (s, J_{CP} = 12.2 Hz), 131.2 (dd, J_{CP} = 9.8 Hz, J_{CH} = 158.7 Hz), 131.8 (dd, J_{CP} = 12.2 Hz, J_{CH} = 161.1 Hz), 132.0 (dd. J_{CP} = 14.6 Hz, J_{CH} = 158.7 Hz), 132.1 (dd, J_{CP} = 12.2 Hz, J_{CH} = 161.1 Hz), 132.5 (dd, J_{CP} = 12.2 Hz, J_{CH} = 158.7 Hz), 133.0 (dd, J_{CP} = 9.8 Hz, J_{CH} = 163.6 Hz), 134.2 (d, J_{CP} = 14.6 Hz), 134.6 (d, J_{CP} = 14.6 Hz; Ph signals; some of the Ph signals are overlapped with the solvent signal), 47.1 (tt, J_{CH} = 126.0 Hz, J_{CP} = 23.2 Hz, CH_2). Anal. Calcd for $C_{42.5}H_{39}O_5P_2ClFeRu_2$ (**8**·0.5CH_2Cl_2): C, 51.82; H, 3.99. Found: C, 51.96; H, 3.90.

Preparation of 9: Successive Reaction of 4 with HBF_4·OEt_2 and H_2SiPh_2. To a CH_2Cl_2 solution (20 mL) of **4** (291 mg, 0.24 mmol) cooled in an ice−water bath was added HBF_4·OEt_2 (0.1 mL, 0.80 mmol), and the resultant mixture was stirred for 1 h at ambient temperature. After removal of the volatiles THF (20 mL) was added to the residue and cooled in an ice−water bath. Then H_2SiPh_2 (0.16 mL, 0.86 mmol) was added to the THF solution and the mixture was stirred for 3 h. Removal of the volatiles under reduced pressure, extraction with Et_2O−hexane (1:2), and separation by alumina column chromatography gave a purple band, from which **9** was isolated as purple crystals (79 mg, 0.08 mmol, 35% yield). **9**: ^1H NMR (C_6D_6) δ_H 7.91−6.58 (20H, m, Ph), 3.74 (2H, br, CH_2); ^{13}C NMR (C_6D_6) δ_C 271.0 (s, μ_3-CO), 202.4, 201.1 (s × 2, Ru−CO), 138.0, 136.1 (t × 2, J = 19.5 Hz, ipso Ph), 132.5, dt, J_{CH} = 161.2 Hz, J_{CP} = 7.3 Hz, Ph signals; other Ph signals were overlapped with the solvent signal), 24.4 (tt, J_{CP} = 18.1 Hz, J_{CH} = 129.4, CH_2P_2). Anal. Calcd for $C_{42}H_{40}O_5P_2FeRu_2$: C, 53.41; H, 4.27. Found: C, 52.98; H, 4.59.

Preparation of 10: Reaction of 4 with $Co_2(CO)_8$. A benzene solution (40 mL) of a mixture of **4** (334 mg, 0.28 mmol) and $Co_2(CO)_8$ (188 mg, 0.55 mmol) was heated for 3 h at 70 °C. After removal of the volatiles under reduced pressure the residue was subjected to alumina column chromatography. Elution with CH_2Cl_2−hexane (1:3−1:0) gave dark red and orange bands. From the former band $Cp^*FeCo(CO)_5$[13] (92 mg, 0.22 mmol, 79% yield) was obtained, and from the latter band **10** (300 mg, 0.27 mmol. 96% yield) was obtained as orange crystals after recrystallization from CH_2Cl_2−hexane. **10**: ^1H NMR (CD_2Cl_2) δ_H 7.45−7.10 (20H, m, Ph), 3.53, 4.12 (dt, $J_{PH} \approx J_{HH} \approx$ 12 Hz, CH_2P_2), 1.83 (15H, s, Cp*). Anal. Calcd for $C_{46.5}H_{38}O_9P_2FeCoRu_2$ (**10**·0.5CH_2Cl_2): C, 48.35; H, 3.22. Found: C, 48.89; H, 3.33.

Experimental Procedure for X-ray Crystallography. Single crystals of **3** (CH_2Cl_2−Et_2O), **4**·(hexane) (Et_2O−hexane), **6**·2(toluene) (CH_2Cl_2−toluene), **8** (THF−hexane), **9** (toluene−hexane), and **10**·2CH_2Cl_2 (CH_2Cl_2−hexane) were obtained by recrystallization from the solvent systems shown in parentheses. Diffraction measurements were made on a Rigaku RAXIS IV imaging plate area detector with Mo Kα radiation (λ = 0.710 69 Å). All the data collections were carried out at −60 °C. The data collections were controlled by software obtained from the Rigaku Corp., Tokyo, Japan (RAXIS (**3**, **4**), RAPID (**6**, **8**−**10**)). Indexing was performed from two oscillation images which were exposed for 4 min. The crystal-to-detector distance was 110 mm. Data collection parameters (detector swing angle (deg)/number of oscillation images/exposure time (min/deg)) were as follows: **3**, 6.0/15/15; **4**·

(13) Akita, M.; Terada, M.; Ishii, N.; Hirakawa, H.; Moro-oka, Y. *J. Organomet. Chem.* **1994**, *473*, 175.

Table 4. Crystallographic Data

	3	**4**·(hexane)	**6**·2(toluene)	**8**	**9**	**10**·$2CH_2Cl_2$
formula	$C_{33}H_{35}O_{10}ClFe_2Ru_2$	$C_{61}H_{66}O_8P_2Fe_2Ru_2$	$C_{68}H_{69}BO_7F_4Fe_2P_2Ru_2$	$C_{42}H_{38}O_5P_2FeRu_2$	$C_{49}H_{47}O_5P_2FeRu_2$	$C_{48}H_{41}O_9Cl_4CoFeP_2Ru_2$
fw	940.90	1302.92	1460.82	942.65	1035.80	1282.47
cryst syst	monoclinic	monoclinic	triclinic	triclinic	triclinic	monoclinic
space group	$P2_1/n$	$P2_1/n$	$P\bar{1}$	$P\bar{1}$	$P\bar{1}$	$P2_1/c$
a/Å	15.920(6)	13.6873(15)	12.623(3)	12.2132(13)	11.3574(8)	11.4541(3)
b/Å	11.8297(12)	13.689(3)	20.931(5)	18.5656(18)	19.0023(14)	19.4961(6)
c/Å	18.874(2)	30.766(3)	12.6338(18)	9.8307(8)	11.3420(6)	22.7347(6)
α/deg			102.959(13)	104.782(7)	104.712(2)	
β/deg	101.139(4	101.511(5)	93.699(12)	112.424(3)	99.917(3)	92.419(2)
γ/deg			100.648(3)	79.310(2	107.112(2)	
V/Å^3	3487.7(14)	5648.5(14)	3177.3(11)	1982.6(3)	2180.5(3)	5072.4(2)
Z	4	4	2	2	2	4
d_{calcd}/g cm^{-3}	1.792	1.532	1.527	1.579	1.578	1.679
μ/mm^{-1}	1.797	1.139	1.029	1.237	1.132	1.513
$2\theta_{max}$/deg	55	55	55	55	55	55
no of params refined	448	656	719	478	542	609
no. of data with $I > 2\sigma(I)$	6149	10 979	5938	7099	7022	8651
total no. of data	6609	11 682	10 777	7728	8897	11 083
R1[a] ($I > 2\sigma(I)$)	0.0486	0.0621	0.0856	0.0779	0.0515	0.0413
wR2[b] (all data)	0.1386	0.1832	0.2114	0.1931	0.1499	0.1270

[a] $R1 = [\sum||F_o| - |F_c||]/\sum|F_o|$ (for data with $I > 2\sigma(I)$). [b] $wR2 = [\sum\{w(F_o^2 - F_c^2)\}^2/\sum\{w(F_o^2)^2\}]^{0.5}$; $w = 1/[\sigma^2(F_o^2)+(0.1000P)^2]$, where $P = [2F_c^2 + \mathrm{Max}(F_o^2,0)]/3$ (for all data).

(hexane), 6.0/22/7.5; **6**·2(toluene), 5.0/36/13.3; **8,** 4.0/45/6.7; **9,** 3.0/60/10.0; **10**·$2CH_2Cl_2$, 3.0/60/8.0. The readout was performed with the pixel size of 100 μm × 100 μm.

Crystallographic data and the results of refinements are summarized in Table 4. The structural analysis was performed on an IRIS O2 computer using the teXsan structure solving program system obtained from the Rigaku Corp., Tokyo, Japan.[14] Neutral scattering factors were obtained from the standard source.[15] In the reduction of data, Lorentz and polarization corrections were made. An absorption correction was also made.[16]

The structures were solved by a combination of direct methods (SHELXS 86)[17] and DIRDIF[18] and refined with the Shelxl97 least-squares refinement program.[17] Unless otherwise stated, non-hydrogen atoms were refined with anisotropic thermal parameters, the methyl hydrogen atoms were refined using the riding models, and the other hydrogen atoms were fixed at calculated positions (C−H = 0.95 Å) and not refined. Details are as follows. **3**: because the bridging hydride ligand could not be located, it was not included in the refinement. **4**: the hexane solvate was refined isotropically, and hydrogen atoms attached to it were not included in the refinement. **6**: the two toluene solvate molecules were refined isotropically, and hydrogen atoms attached to them were not included in the refinement. **9**: the toluene solvate was found to be disordered and refined, taking into account two components ((C91−97):(C101−107) = 0.51:0.49). Hydrogen atoms attached to it were not included in the refinement.

Acknowledgment. We are grateful to the Yamada Science Foundation for financial support of this research. We are grateful to Mr. Satoshi Kakuta and Prof. Hiroharu Suzuki (Tokyo Institute of Technology) for the 2D NMR measurements.

Supporting Information Available: Tables giving crystallographic results for **3**, **4**, **6**, and **8**−**10**. This material is available free of charge via the Internet at http://pubs.acs.org.

OM020722U

(14) teXsan: Crystal Structure Analysis Package, version 1.11; Rigaku Corp., Tokyo, Japan, 2000.

(15) *International Tables for X-ray Crystallography*; Kynoch Press: Birmingham, U.K., 1975; Vol. 4.

(16) Higashi, T. Program for Absorption Correction; Rigaku Corp., Tokyo, Japan, 1995.

(17) (a) Sheldrick, G. M. SHELXS-86: Program for Crystal Structure Determination; University of Göttingen, Göttingen, Germany, 1986. (b) Sheldrick, G. M. SHELXL-97: Program for Crystal Structure Refinement; University of Göttingen, Göttingen, Germany, 1997.

(18) Beurskens, P. T.; Admiraal, G.; Beurskens, G.; Bosman, W. P.; Garcia-Granda, S.; Gould, R. O.; Smits, J. M. M.; Smykalla, C. The DIRDIF Program System, Technical Report of the Crystallography Laboratory; University of Nijmegen, Nijmegen, The Netherlands, 1992.